Conformational Variation Revealed by the Crystal Structure of RNase U2A Complexed with Ca Ion and 2'-Adenylic Acid at 1.03 Å Resolution

Shuji Noguchi

Graduate School of Pharmaceutical Sciences, The University of Tokyo, Tokyo 113-0033, Japan

Corresponding author: Shuji Noguchi; 7-3-1 Hongo, Bunkyo-ku, Tokyo 113-0033, Japan; E-mail: snoguchi@mol.f.u-tokyo.ac.jp; Tel: +81-3-5841-4842; Fax: +81-3-5841-4891.

Running title: Conformational Variation of RNase U2A.

Abstract: Asparagine can be non-enzymatically deamidated and isomerized *via* succinimide to isoaspartate. This post-translational modification can potentially alter the physical properties or the function of the parent protein. Asn32 of ribonuclease U2A from *Ustilago sphaerogena* is known to rapidly deamidate and isomerize in alkaline conditions. The crystal structure of ribonuclease U2A complexed with 2'-adenylic acid and calcium ions was determined at 1.03 Å resolution. In this structure, the region from Asp29 to Asp37 winds around a calcium ion, and the main-chain of Asn32–Gly33 adopts an extended conformation. Rotation of the side-chain of Asn32 could bring Asn32C_γ into close proximity to Gly33N, in a conformation suitable for succinimide formation. The structure suggests that in solution the region around Asn32–Gly33 is likely to be in equilibrium between multiple conformers, with the deamidation of Asn32 proceeding when the region adopts an extended conformation.

Key words: Asparagine deamidation; Isoaspartate; Isomerization; Ribonuclease U2; Succinimide; *Ustilago sphaerogena*.

INTRODUCTION

Asparagine can be non-enzymatically deamidated and isomerized to isoaspartate (isoAsp) *via* succinimide in proteins and peptides [1, 2] (Fig. 1). The chemical and three-dimensional structural changes induced by this post-translational modification *in vivo* can cause dysfunction or changes in physical properties such as solubility of proteins [2–4. These changes can in turn result in diseases as suggested by the fact that accumulation of proteins containing isoAsp *in vivo* is fatal [5]. The rate of deamidation and isoAsp formation depends on the local amino acid sequence, especially on the C-terminal side of Asn, and is fastest in the Asn-Gly sequence [6]. In the case of folded proteins, the rate is expected to depend also on the conformation of the region around Asn. Ribonuclease (RNase) U2, a purine-specific endo-ribonuclease secreted from smut fungus *Ustilago sphaerogena* [7], has been used in structural studies of isoAsp formation in proteins [8-10]. The deamidation and isomerization to isoAsp is reported to occur rapidly to RNase U2 Asn32–Gly33 under alkaline conditions [11]. Although the crystal structures of RNase U2 containing Asn32 complexed with 3'-adenylic acid (3'-AMP; PDB ID 3AGN and 3AGO) suggest that the region around Asn32-Gly33 is flexible, nucleophilic attack of Gly32N on Asn32C_{γ}, which is the first step in Asn deamidation, seems likely to be difficult due to steric hindrance [9, 10]. Therefore, the mechanism of Asn32 deamidation in RNase U2 remains somewhat obscure. We report here the crystal structure of RNase U2 containing Asn32 (U2A) complexed with calcium ions and the inhibitor adenosine 2'-adenylic acid (2'-AMP) at 1.03 Å resolution. The structure allows inference of the likely mechanism of deamidation at Asn32 of RNase U2.

MATERIALS AND METHODS

RNase U2A was purified from the culture broth of *U. sphaerogena* by the method of Uchida and Shibata [12]. The crystals were grown by the hanging-drop vapor-diffusion method in the modified condition as described previously [13]. The protein solution containing RNase U2A 20 mg/mL and 20 mM 2'-AMP, adjusted to pH 6 with NaOH, was mixed with the equal volume of solution A consisting of 18% (w/v) polyethylene glycol 8000, 200 mM calcium acetate, 100 mM sodium cacodylate, pH 6.5, and equilibrated over solution A at 293K. The clusters of the crystals appeared with in 2 days. Crystal seeds from the clusters were transferred with the streak seeding method to the droplet mixture of 3 μl protein solution and 5 μl solution A equilibrated over solution A for 2 days at 293K. The single crystals of a plate shape grew up to 0.35×0.35×0.05 mm^3 within 5 days. The crystal parameters are summarized in Table 1, together with the statistics of the X-ray diffraction data collection and crystallographic refinement.

The crystal was cryoprotected by soaking it in solution A containing 5, 10, 15, and 20% (v/v) glycerol sequentially for approximately ten seconds each and was flash-frozen in a stream of N_2 at 95 K. X-ray diffraction data collection was carried out at beamline 6A at KEK Photon Factory (Tsukuba, Japan). Diffraction images were processed with the HKL2000 package [14]. The crystal structure was determined by the molecular replacement method using MOLREP implemented in CCP4 package [15], with the crystal structure of RNase U2A complexed with adenosine 3'-monophosphate (3'-AMP; Protein Data Bank (PDB) code 3AGN) as a search model. Crystallographic refinements were performed using REFMAC5 [16], and the manual revision of the structural model was performed using Coot

[17]. Atomic displacement parameters (*B*-factors) of the individual atoms were refined anisotropically after the resolution of the refinement was extended to 1.30 Å. The hydrogen atoms generated at their riding positions were included in the model after the resolution was extended to 1.10 Å resolution. The quality of the refined models were assessed by RAMPAGE [18]. The atomic coordinates and experimental structure amplitudes had been deposited in the PDB with the code 3AHW.

RESULTS AND DISCUSSION

The asymmetric unit contains one RNase U2A molecule (Fig. 2). All the amino acid residues and the bound 2'-AMP were defined in the electron density maps. The bound 2'-AMP adopts a *syn*-conformation about a glycosyl bond and shows a $C_{2'}$-*endo* ribose pucker. The phosphate moiety of 2'-AMP is located at the catalytic site, and is hydrogen-bonded to the active site residues [8] Tyr39, His41, Glu62, Arg85, and His101. The adenine base of 2'-AMP is not bound to the adenine-recognition site observed in 3AGN and 3AGO structures but to the less-specific base-binding subsite near His101 [8, 19, 20]. This suggests that RNase U2A cannot recognize the adenine base at pH 6.5, a pH at which RNase U2A is catalytically inactive [7].

As compared to 3AGN and 3AGO structures, a conformational difference is found in the region from Asp29 to Asp37. This region, which adopts an α-helical conformation in the 3AGN structure, is unfolded, and instead winds around a calcium ion. Asp29$O_{\delta1}$, Val30O, Asn32$O_{\delta1}$, and Asp37$O_{\delta2}$ are coordinated to the calcium ion in a square planar geometry at distances of 2.31 Å, 2.31 Å, 2.27 Å, and 2.34 Å, respectively, (Fig. 3). Two water molecules are

also coordinated to the calcium ion perpendicular to the plane at slightly longer distances of 2.38 Å and 2.39 Å. Thus the six coordinating atoms are in an octahedral geometry that is elongated along the bonds between the water molecules and the calcium ion. The region from Val30 to Gly33 is in an extended conformation. An approximately 110° rotation of the side-chain torsion angle χ_1 of Asn32 would bring Asn32C_γ into close proximity, approximately 3 Å, with Gly33N. This side-chain rotation would enable nucleophilic attack of Gly33N on Asn32C_γ, which is the first step of the deamidation reaction. In solution, the region from Val30 to Gly33 of RNase U2A may be in equilibrium between the α-helical conformation and the unfolded, extended conformation observed in the crystal structure and shown in Fig. 2. Deamidation of Asn32 would proceed when this region is in the extended conformation, which is suitable for succinimide formation. The structural change caused by the deamidation and isomerization of Asn could interfere with the functions of protein biopharmaceuticals [2]. The flexibility of regions containing the labile sequence Asn-Gly should be taken into the consideration in designing biopharmaceuticals to prevent formation of modified species containing isoAsp.

ACKNOWLEDGMENTS

This work was supported by a Grant-in-Aid for Scientific Research to SN (No.07772128) from the Ministry of Education, Science, Sports, and Culture, Japan. The synchrotron radiation experiments were performed under the approval of the Photon Factory Program Advisory Committee (Proposal No. 2008G141).

REFERENCES

[1] Geiger, T.; Clarke, S. Deamidation, isomerization, and racemization at asparaginyl and aspartyl residues in peptides. Succinimide-linked reactions that contribute to protein degradation. *J. Biol. Chem.,* **1987**, *262*, 785–794.

[2] Manning, M.C.; Chou, D.K.; Murphy, B.M.; Payne, R.W.; Katayama, D.S. Stability of protein pharmaceuticals: an update. *Pharm. Res.,* **2010**, *27*5, 44–575.

[3] Shimizu, T.; Watanabe, A.; Ogawara, M.; Mori, H.; Shirasawa, T. Isoaspartate formation and neurodegeneration in Alzheimer's disease. *Arch. Biochem. Biophys.,* **2000**, *381*, 225–234.

[4] Miyawaki, K.; Noguchi, S.; Harada, S.; Satow, Y. *J. Cryst. Growth,* **1996**, *168*, 292–296.

[5] Kim, E.; Lowenson, J.D.; MacLaren, D.C.; Clarke, S.; Young, S.G. Deficiency of a protein-repair enzyme results in the accumulation of altered proteins, retardation of growth, and fatal seizures in mice. *Proc. Natl. Acad. Sci. USA,* **1997**, *94*, 6132–6137.

[6] Stephenson, R.C.; Clarke, S. Succinimide formation from aspartyl and asparaginyl peptides as a model for the spontaneous degradation of proteins. *J. Biol. Chem.,* **1989**, *264*, 6164–6170.

[7] Arima, T.; Uchida, T.; Egami, F. Studies on extracellular ribonucleases of *Ustilago sphaerogena*. Purification and properties. *Biochem. J.,* **1968**, *106*, 601–607.

[8] Noguchi, S.; Satow, Y.; Uchida, T.; Sasaki, C.; Matsuzaki, T. Crystal structure of *Ustilago sphaerogena* ribonuclease U2 at 1.8 Å resolution. *Biochemistry*, **1995**, *34*, 15583–15591.

[9] Noguchi, S. Isomerization mechanism of aspartate to isoaspartate implied by structures of *Ustilago sphaerogena* ribonuclease U2 complexed with adenosine 3'-monophosphate. *Acta Crystallogr. Sect. D Biol. Crystallogr.,* **2010**, *66*, 843–849.

[10] Noguchi, S. Structural changes induced by the deamidation and isomerization of asparagine revealed by the crystal structure of *Ustilago sphaerogena* ribonuclease U2B. *Biopolymers*, **2010**, *93*, 1003–1010.

[11] Kanaya, S.; Uchida, T. Comparison of the primary structures of ribonuclease U2 isoforms. *Biochem. J.,* **1986**, *240*, 163–170.

[12] Uchida, T; Shibata, Y. An affinity adsorbent, 5'-adenylate-aminohexyl-sepharose. I. Purification and properties of two forms of RNase U2. *J. Biochem.,* **1981**, *90*, 463–471.

[13] Noguchi, S.; Satow, Y.; Uchida, T.; Sasaki, C.; Matsuzaki, T. *J. Cryst. Growth,* **1996**, *168*, 270–274.

[14] Otwinowski, Z.; Minor, W. Processing of X-ray diffraction data collected in oscillation mode. *Method Enzymol.,* **1997**, *276*, 307–326.

[15] CCP4. The CCP4 suite: programs for protein crystallography. *Acta Crystallogr. Sect. D Biol. Crystallogr.,* **1994**, *50*, 760–763.

[16] Murshudov, G.N.; Vagin, A.A.; Dodson, E.J. Refinement of macromolecular structures by the maximum-likelihood method. *Acta. Crystallogr. Sect. D Biol. Crystallogr.,* **1997**, *53*, 240–255.

[17] Emsley, P.; Cowtan, K. Coot: model-building tools for molecular graphics. *Acta Crystallogr. D Biol. Crystallogr.,* **2004**, *60*, 2126–2132.

[18] Lovell, S.C.; Davis, I.W.; Arendall, W.B.; de Bakker, P.I.; Word, J.M.; Prisant, M.G.; Richardson, J.S.; Richardson, D.C. Structure validation by C_α geometry: φ, ψ and C_β deviation. *Proteins,* **2003**, *50*, 437–450.

[19] Yasuda, T.; Inoue, Y.; Studies of catalysis by ribonuclease U2. Steady-state kinetics for transphosphorylation of oligonucleotide and synthetic substrates. *Biochemistry*, **1982**, *21*, 364–369.

[20] Granzin, J.; Puras-Lutzke, R.; Landt, O.; Grunert, H.P.; Heinemann, U.; Saenger, W.; Hahn, U. RNase T1 mutant Glu46Gln binds the inhibitors 2'GMP and 2'AMP at the 3' subsite. *J. Mol. Biol.,* **1992**, *225*, 533–542.

Figure legend

Figure 1. Reaction pathway for deamidation and isomerization of asparagine.

Figure 2. Stereo view of the overall structures of RNase U2A. The C_α-traces of RNase U2A complexed with 2'-AMP (thick black line) and those with 3'-AMP (3AGN, thick gray line; 3AGO, thin black line) were superposed using main-chain atoms. The side chains of Asn32, the bound 2'-AMP and 3'-AMP molecules are shown as stick models. Four calcium ions bound to RNase U2A complexed with 2'-AMP are shown as white spheres. Asp29 and Asp37 are labeled with their residue numbers.

Figure 3. The calcium binding site near Asp29–Asp37. C, N, and O atoms are shown in black, gray, and white, respectively, and Ca ion as white sphere. Coordination bonds and hydrogen bonds are shown in dashed black lines.

Table 1. X-ray diffraction data collection and refinement summary.

Crystal parameter	
Space group	$P2_1$
Unit cell parameters (Å, °)	a = 38.994, b = 35.940, c = 36.151, β = 103.42
Data collection statistics	
Wavelength (Å)	0.978
Resolution range (Å)	25.14 - 1.03 (1.06-1.03)
No. of unique reflections	47871 (3337)
Completeness (%)	99.2 (93.9)
Multiplicity	6.5 (3.0)
Mean $I/\sigma(I)$	36.2 (2.2)
R_{merge}(%)	9.3 (39.5)
Refinement statistics	
R_{work} / R_{free} (%)	13.7/14.4 (35.9/36.2)
No. of atoms (non-H)	
Protein	905
Ligand / Ion	27
Water	158
R.m.s. deviations	
Bond lengths (Å)	0.012
Bond angles (°)	1.656
Average B-factors (Å^2)	10.7
Ramachandran statistics	
Favored (%)	98.2
Allowed (%)	1.8
Outliers	None

Values in parentheses are for the highest resolution shell.

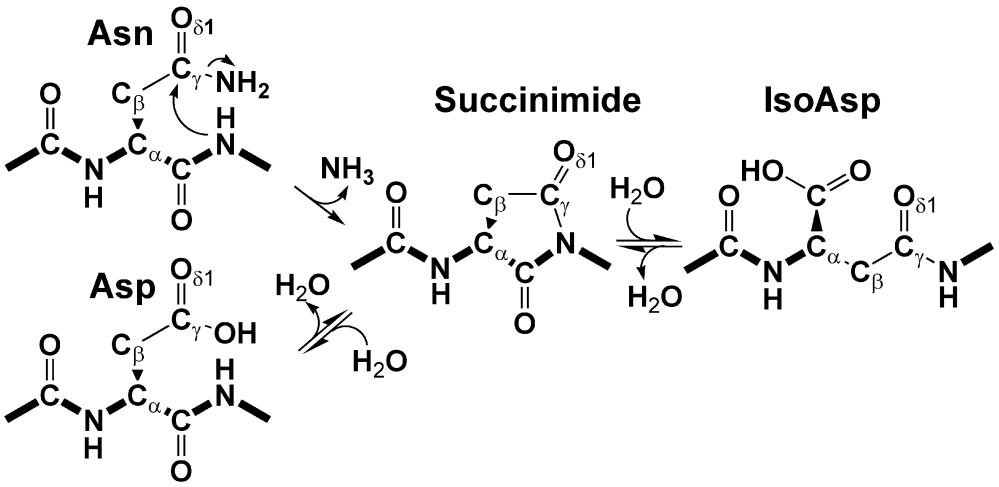

Figure 1.

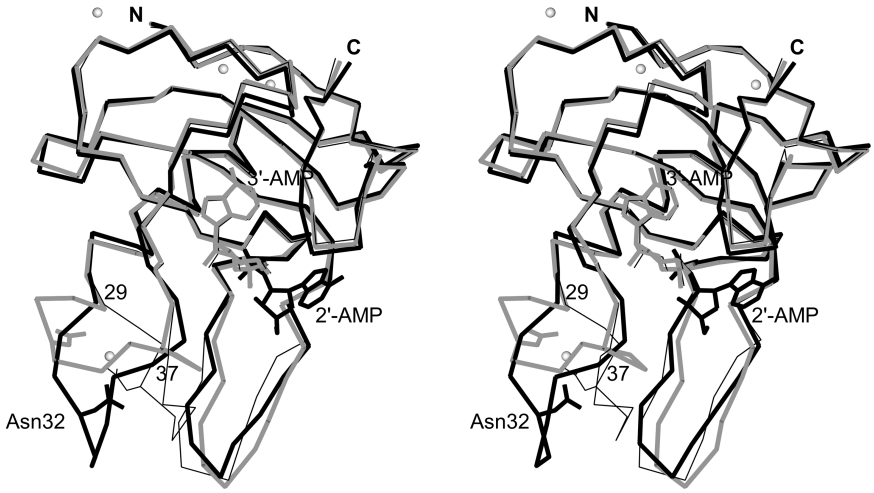

Figure 2.

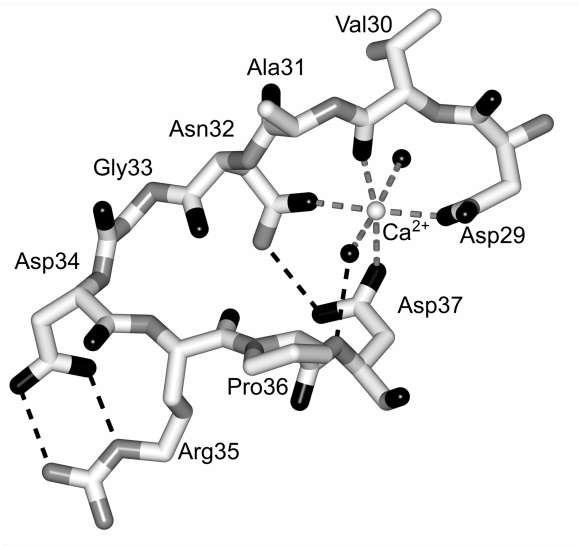

Figure 3.